Transition from anomalous to normal hysteresis in a system of coupled Brownian motors: A mean-field approach

S. E. Mangioni and R. R. Deza
Departamento de Física, FCEyN, Universidad Nacional de Mar del Plata, Deán Funes 3350, 7600 Mar del Plata, Argentina

H. S. Wio
Centro Atómico Bariloche (CNEA) and Instituto Balseiro (CNEA and UNCuyo), 8400 San Carlos de Bariloche, Argentina
(Received 28 September 2000; published 29 March 2001)

We address a recently introduced model describing a system of periodically coupled nonlinear phase oscillators submitted to *multiplicative* white noises, wherein a ratchetlike transport mechanism arises through a symmetry-breaking noise-induced nonequilibrium phase transition. Numerical simulations of this system reveal amazing novel features such as *negative zero-bias conductance* and *anomalous hysteresis*, explained by performing a strong-coupling analysis in the thermodynamic limit. Using an explicit mean-field approximation, we explore the whole ordered phase finding a transition from anomalous to normal hysteresis inside this phase, estimating its locus, and identifying (within this scheme) a mechanism whereby it takes place.

DOI: 10.1103/PhysRevE.63.041115 PACS number(s): 05.40.−a, 87.10.+e, 82.40.Bj

I. INTRODUCTION

Feynman's ratchet-and-pawl example [1], illustrating the impossibility for a microscopic rectifying device to extract work in a cyclic manner from the *equilibrium* fluctuations of a *single* heat bath, spurred in turn the search for heat engines operating in a *far from equilibrium* regime between *two* heat baths. The field of ''nanomechanics'' (more specifically, that of noise-induced transport or ''Brownian motors'') is now about one decade old [2]. In the early works, a requisite for these devices to operate (besides their obvious built-in, ratchetlike bias) seemed to be that the fluctuations be correlated [3]. That requirement was relaxed when ''pulsating'' ratchets were discovered: in these it is the random *switching* between uncorrelated noise sources that is responsible of the rectifying effect [4].

A recent new twist has been to relax also the requirement of a built-in bias [5]: a system of periodically coupled nonlinear phase oscillators in a symmetric ''pulsating'' environment has been shown to undergo a noise-induced nonequilibrium phase transition, wherein the spontaneous symmetry breakdown of the stationary probability distribution gives rise to an *effective* ratchetlike potential. The authors introduced the aforementioned mechanism and its striking consequences, such as the appearance of *negative zero-bias conductance* and *anomalous hysteresis*, which they illustrated through numerical simulations and explained by using the strong-coupling limit. By anomalous hysteresis, we refer to the case in which the cycle runs clockwise, contrary to the normal one (as typified by a ferromagnet), which runs counterclockwise.

Exploiting our previous experience in a lattice model displaying (like the present one) a symmetry-breaking nonequilibrium phase transition [6] and in order to set a firm basis for further work, we addressed the model using an explicit mean-field approach [7], focusing on the relationship between the *shape* of the stationary probability distribution (as well as the *number of solutions* to the mean-field equations) and the transport properties in its different regions. Hence it is our aim in this work to report on the thorough exploration of the ordered phase, on the characterization of its subregions, and on features related to the transition from anomalous to normal hysteresis in the behavior of the particle current as a function of the bias force. Our main finding is that there exists a close relationship between the character of the hysteresis loop on the one hand, and the shape of the stationary probability distribution as well as the number of ''homogeneous'' solutions (a term to be clarified later) on the other.

In the following sections, we successively introduce the model, describe the mean-field approach, discuss our numerical results, and draw our conclusions. For the benefit of the reader, we have included an Appendix in which some (in our judgment) subtle calculations are performed in some detail.

II. THE MODEL

In Ref. [5], the authors consider a set of *globally* coupled stochastic equations of motion (in the overdamped regime, and to be interpreted in the sense of Stratonovich) for the N degrees of freedom (phases) $X_i(t)$:

$$\dot{X}_i = -\frac{\partial U_i}{\partial X_i} + \sqrt{2T}\xi_i(t) - \frac{1}{N}\sum_{j=1}^{N} K(X_i - X_j). \qquad (1)$$

The model just set up can be visualized (at least for some parameter values) as a set of overdamped interacting pendula. The second term models, as usual, the effect of thermal fluctuations: T is the temperature of the environment and the $\xi_i(t)$ are *additive* Gaussian white noises with zero mean and variance 1,

$$\langle \xi_i(t) \rangle = 0, \quad \langle \xi_i(t)\xi_j(t') \rangle = \delta_{ij}\delta(t-t'). \qquad (2)$$

The ''pulsating'' potentials $U_i(x,t)$ are among the key ingredients in the model [4] ($x \in [-L/2, L/2]$ is a phaselike real variable that runs over the range of $X_i(t)$, namely the allowed values for any realization of any X_i at any time t). They consist of a static part $V(x)$ and a fluctuating one: Gaussian white noises $\eta_i(t)$ with zero mean and variance 1 [i.e., obeying also Eq. (2) but assumed *nonthermal* in origin]

are coupled *multiplicatively* (with intensity Q) through a function $W(x)$. Even though we adopted $L=2\pi$ in all our numerical calculations, we kept in all the equations the dependence on L in order to have the most general expressions. For an analysis of the noise-induced ratchet effect, a ''load force'' F, producing an additional bias, is also included,

$$U_i(x,t)=V(x)+W(x)\sqrt{2Q}\,\eta_i(t)-Fx. \tag{3}$$

As already stated, both $V(x)$ and $W(x)$ are assumed to be *periodic* (period L) and moreover they are *symmetric*:

$$V(-x)=V(x), \quad W(-x)=W(x),$$

which means that there is no *built-in* ratchet effect. In Ref. [5], the choice was

$$V(x)=W(x)=-\cos x-A\cos 2x, \tag{4}$$

with $A>0$ so as to remove an accidental degeneracy hindering the spontaneous symmetry breakdown [5], but not strong enough to create a local minimum at $L/2=\pi$. With the choice $A>0$, the direction of the particle current $\langle\dot{X}\rangle$ turns out to be *opposite* to that of symmetry breaking in the stationary probability distribution $P^{st}(x)$, and it is this effect that leads in turn to such oddities as *negative zero-bias conductance* and *anomalous hysteresis* [5] (a nice animation illustrating this phenomenon can be found on the web [8]).

The interaction force $K(x-y)=-K(y-x)$ between oscillators (the other key ingredient in the model) is also assumed to be a *periodic* function of $x-y$ with the same period $L=2\pi$ as $V(x), W(x)$. In Ref. [5], it is

$$K(x)=K_0\sin x, \quad K_0>0. \tag{5}$$

As indicated before, the model can be visualized (at least for $A\to 0$) as a set of overdamped and interacting pendula (only their phases matter, not their locations) interacting with one another through a force proportional to the sine of their phase difference (a force that is always attractive in the reduced interval $-\pi\leqslant x-y\leqslant\pi$).

Summarizing, the complete set of parameters in the model is N, F, T, A, K_0, and Q. Except for numerical simulations, the exact value of N is unimportant, as long as it is large. As already said, F is just an auxiliary tool for the analysis. We shall fix the values of T and A as in Ref. [5], namely $T=2$, $A=0.15$. So the important parameters in the model are K_0 (governing mostly the ''drift'' terms in this set of generalized Langevin equations) and Q (governing mostly the ''diffusion'' ones). As discussed in Ref. [4], the Gaussian character of $\eta_i(t)$ allows it to be added to $\xi_i(t)$. Hence it suffices to consider the $\eta_i(t)$'s, now coupled through $S(x)\equiv\sqrt{2}[T+Q(W')^2]^{1/2}$ [note that $S(x)=\sqrt{2}g(x)$ as defined in Ref. [5]].

III. MEAN-FIELD ANALYSIS

On account of the choice made in Eq. (4), the interparticle interaction term in Eq. (1) can be cast in the form

$$\frac{1}{N}\sum_{j=1}^{N}K(X_i-X_j)=K_0[C_i(t)\sin X_i-S_i(t)\cos X_i]. \tag{6}$$

For $N\to\infty$, we may approximate Eq. (1) in the manner of Curie-Weiss, replacing $C_i(t)\equiv N^{-1}\Sigma_j\cos x_j(t)$ and $S_i(t)\equiv N^{-1}\Sigma_j\sin x_j(t)$ by $C_m\equiv\langle\cos x_j\rangle$ and $S_m\equiv\langle\sin x_j\rangle$, respectively, to be determined as usual by self-consistency. This decouples the system of stochastic differential equations (SDE) in Eq. (1), which reduces to essentially one Markovian SDE for the single stochastic process $X(t)$:

$$\dot{X}=R(X)+S(X)\,\eta(t), \tag{7}$$

with

$$\begin{aligned}R(x)&=-V'(x)+F-K_m(x)\\&=-\sin x(1+K_0C_m+4A\cos x)+K_0S_m\cos x+F\end{aligned} \tag{8}$$

(where $K_m(x)=K_0[C_m\sin x-S_m\cos x]$) and

$$\begin{aligned}S(x)&=\sqrt{2\{T+Q[W'(x)]^2\}}\\&=\sqrt{2\{T+Q[\sin x+2A\sin 2x]^2\}},\end{aligned} \tag{9}$$

so that the ''spurious'' contribution to the drift in the Stratonovich interpretation is

$$\frac{1}{2}S(x)S'(x)=QW'(x)W''(x)=Q(\sin x+2A\sin 2x)(\cos x+4A\cos 2x). \tag{10}$$

We may write $R(x)=-\mathcal{V}'(x)$ in terms of an *effective* [since C_m and S_m are determined by self-consistency in terms of $P^{st}(x)$ below] and moreover by the asymmetric (hence ratchetlike) potential

$$\begin{aligned}\mathcal{V}(x)&=V(x)+\int_0^x K_m(y)dy-Fx\\&=-[\cos x(1+K_0C_m)+A\cos 2x]-K_0S_m\sin x-Fx.\end{aligned}$$

Similarly, $S(x)S'(x)/2$ can be derived from $-Q[W'(x)]^2/2$.

A. The stationary probability distribution function

The Fokker-Planck equation associated with the SDE in Eq. (7) is

$$\begin{aligned}\partial_tP(x,t)&=\partial_x\{-[R(x)+\tfrac{1}{2}S(x)S'(x)]P(x,t)\}\\&\quad+\tfrac{1}{2}\partial_{xx}[S^2(x)P(x,t)]\end{aligned} \tag{11}$$

[see the Appendix, Eqs. (A3) and (A4)] and its normalized stationary solution *with periodic boundary conditions* and current density $J\neq 0$ is [4,5]

$$P^{st}(x)=\frac{e^{-\phi(x)}H(x)}{\mathcal{N}S(x)}, \tag{12}$$

where

$$\phi(x) = -2\int_0^x dy\,\frac{R(y)}{S^2(y)}, \tag{13}$$

$$H(x) = \int_x^{x+L} dy\,\frac{\exp[\phi(y)]}{S(y)}, \tag{14}$$

and $\mathcal{N} = \int_{-L/2}^{L/2} dx\, P^{st}(x)$. The positive sign of $S(x)$ and the exponentials implies that of $H(x)$ and hence that of $P^{st}(x)$ and $\mathcal{N}$, as it should be. On the other hand, although $R(x)$, $S(x)$, and $P^{st}(x)$ are periodic by construction, $\phi(x)$ is not required to be so; in fact, it increases on each cycle by an amount

$$\phi(L) = \frac{1}{T}\int_0^L \frac{dx\,p(x)\sin x}{q(x)} - \frac{K_0 S_m}{T}\int_0^L \frac{dx\cos x}{q(x)} - \frac{F}{T}\int_0^L \frac{dx}{q(x)}, \tag{15}$$

with $p(x) = 1 + K_0 C_m + 4A\cos x$ and $q(x) = 1 + (Q/T)\sin^2 x(1+4A\cos x)^2$, both even functions of x. Since only the first term vanishes identically, for nonzero F or S_m it will be the case *generically* that $\phi(L) \neq 0$; thus the form of $H(x)$ in Eq. (14) is designed to compensate for this fact. Moreover (as shown in the Appendix) for $A > 0$, $[q(x)]^{-1}$ (>0) gives less weight to the positive $\cos x$ values than to the negative ones, and it does increasingly so the larger Q is; hence the two nonzero contributions to $\phi(L)$ compete with each other.

According to Eq. (A15) in the Appendix,

$$J = [1 - e^{\phi(L)}]/2\mathcal{N}, \tag{16}$$

hence the sign of J is that of $1 - e^{\phi(L)}$ and—on the other hand—the ''holonomy'' condition $e^{\phi(L)} = 1$ implies $J = 0$ and $H(x) = \text{const}$ [see the Appendix, Eq. (A8)]. Equation (16) is a self-consistency relation since both $\mathcal{N}$ and $\phi(L)$ keep information on the shape of $P^{st}(x)$ (in the latter case through C_m and S_m). A nonzero J is always associated with a symmetry breakdown in $P^{st}(x)$ [namely, $P^{st}(-x) \neq P^{st}(x)$]. This may be either *spontaneous* (our main concern here) or *induced* by a nonzero F.

B. The self-consistency equations

As indicated earlier, the stationary probability distribution $P^{st}(x)$ depends on both S_m and C_m, since $R(x)$ includes $K_m(x)$. Their values arise from requiring self-consistency, which amounts to solving the following system of nonlinear integral equations:

$$F_{cm} = C_m \quad \text{with}$$

$$F_{cm} \equiv \langle \cos x \rangle = \int_{-L/2}^{L/2} dx\,\cos x\, P^{st}(x, C_m, S_m), \tag{17}$$

$$F_{sm} = S_m \quad \text{with}$$

$$F_{sm} \equiv \langle \sin x \rangle = \int_{-L/2}^{L/2} dx\,\sin x\, P^{st}(x, C_m, S_m). \tag{18}$$

These equations give C_m and S_m for each set of the parameters (Q, K_0) that define the state of the system (assuming T, A, and F fixed).

For $F = 0$, the choice $S_m = 0$ makes $R(x)$ in Eq. (8) an odd function of x; this in turn makes $\phi(x)$ in Eq. (13) even, and then the periodicity of $P^{st}(x)$ in Eq. (12) [in the form $P^{st}(-x) = P^{st}(-x-L)$] implies that the stationary probability distribution is also an even function of x. So the problem of self-consistency reduces to the *numerical* search of solutions of Eq. (17), with $S_m = 0$. Nonetheless, a plausibility argument leads to some intuition on the existence of some solutions of this integral equation (and their stability) in this symmetric case.

(i) Since—as argued—$J = 0$ and $H(x) = \text{const}$ holds, it turns out from Eq. (11) that the set of critical points x_c of $P^{st}(x)$ must obey $R(x_c) = \frac{1}{2} S(x_c) S'(x_c)$.

(ii) Since $x_c = 0, \pi (\text{mod}\, 2\pi)$ belong to that set, a possible way to satisfy the integral equation in Eq. (17) is for $P^{st}(x)$ to be concentrated around those values.

(iii) Then, by analogy with a pendulum, one expects the solution with $C_m > 0$ to be the stable one for K_0/Q large enough (what we shall call an ''interaction-driven regime'' or IDR). For K_0/Q small enough (''noise-driven regime'' or NDR) the stable solution *can* have $C_m < 0$ (implying an ''angle'' larger than $\pi/2$ with respect to the mean field) since it corresponds to shaking the pendula violently.

Beyond these handwaving arguments, it must be said that, since $\cos x$ in Eq. (17) is an even function of x, in order to determine the stability of the true solutions it suffices to use the Curie-Weiss (i.e., the one-parameter) criterion, namely to check whether the slope at S_m of the integral in Eq. (18) is less than or greater than 1. As a complementary check, a small-x expansion of $\phi(x)$ (see the Appendix) confirms that $P^{st}(x)$ is indeed Gaussian at $x = 0$. For *small* $F \neq 0$, $P^{st}(x)$ gets multiplied (in this approximation) by $\exp[Fx/T] (\approx 1 + Fx/T)$, which leads to a nonzero value of $S_m = kF$ with $k > 0$. By the mechanism discussed after Eq. (15), for Q large enough, $\phi(L) > 0$ and by Eq. (16), $J < 0$. As will be shown later, this effect manifests itself in a *negative zero-bias conductance*.

We conclude that for $F = 0$ there are always one or more solutions to Eqs. (17) and (18) with $S_m = 0$ and one of these is the stable one in the ''disordered'' phase. As argued in Ref. [5], for $N \to \infty$ a noise-induced nonequilibrium transition takes place *generically* towards an ''ordered'' phase where $P^{st}(-x) \neq P^{st}(x)$. In the present scheme, this asymmetry should be evidenced by the fact that the solution with $S_m = 0$ becomes unstable in favor of two other solutions such that $P_2^{st}(x) = P_1^{st}(-x)$, characterized by *nonzero* values $\pm|S_m|$. This fact confers upon S_m the character of an order parameter.

C. The phase boundary

Since $\sin x$ is an antisymmetric function, Eq. (18) turns out to be impractical for the task of finding the curve that

separates the ordered phase from the disordered one, given that on that curve S_m is still zero. For that goal (exclusively) we solve, instead of Eqs. (17) and (18), the following system:

$$\int_{-L/2}^{L/2} dx \cos x P^{st}(x, C_m, 0) = C_m , \tag{19}$$

$$\int_{-L/2}^{L/2} dx \sin x \frac{\partial P^{st}}{\partial_{S_m}}|_{S_m=0} = 1. \tag{20}$$

D. The particle current

The appearance of a ratchet effect amounts to the existence of a nonvanishing drift term $\langle \dot{X} \rangle$ in the stationary state, in the absence of any forcing ($F=0$); in other words, the pendula become rotators in an average sense. As discussed above, the cause of this spontaneous particle current is the noise-induced asymmetry in $P^{st}(x)$ [5].

As is shown in the Appendix,

$$\langle \dot{X} \rangle = \int_{-L/2}^{L/2} dx \left[R(x) + \frac{1}{2} S(x) S'(x) \right] P^{st}(x, C_m, S_m), \tag{21}$$

and the final result is

$$\langle \dot{X} \rangle = JL = \left\{ \frac{1 - e^{\phi(L)}}{2\mathcal{N}} \right\} L. \tag{22}$$

Hence $\langle \dot{X} \rangle$ has the sign of J and can be also regarded as an order parameter. In fact, from Eqs. (8) and (21)—or equivalently from Eqs. (8), (13), and (22)—one may suspect the existence of a close relationship between $\langle \dot{X} \rangle$ and S_m.

IV. NUMERICAL RESULTS

Figure 1 displays (on the same scale as Fig. 1b of Ref. [5], with which it fully coincides) the phase diagram obtained by solving Eqs. (19) and (20) using the Newton-Raphson method. In the region above the full line (''ordered region''), the stable solution to Eqs. (17) and (18) has $S_m \neq 0$. Notice that this noise-induced phase transition is *reentrant*: as Q increases for $K_0 = \text{const}$, the ''disordered phase'' ($S_m = 0$) is met again. The multiplicity of mean-field solutions in the ordered region, together with the fact that some of them may suddenly disappear as either K_0 or Q are varied (a fact that, as we shall see, is closely related to the occurrence of anomalous hysteresis) hinders the pick of the right solution in this region.

A more systematic characterization of the aforementioned multiple solutions is achieved when the branch to which they belong is followed from its corresponding ''homogeneous'' ($S_m = 0$) solution. Accordingly, the dashed line in Fig. 1 separates two sectors within the ordered region with regard to the *homogeneous* solutions. Below it (''noise-driven regime'' or NDR) there is *a single* solution with $S_m = 0$ and $C_m < 0$ (as already suggested, in this regime a solution with $C_m < 0$ *can* be stable since it corresponds to shaking the pendula violently). Above it (''interaction-driven regime'' or IDR) there are *three*: two of them have opposite signs and (for K_0/Q large enough) $|C_m| \simeq 0.9$; the remaining one has $C_m \approx 0$. Note that this line presents a dip, whose meaning will be discussed in relation to the character of the hysteresis loop. We have studied the shape of $P^{st}(x)$ and the behavior of $\langle \dot{X} \rangle$ as a function of F for different locations in this (Q, K_0) diagram. The squares in Fig. 1 indicate several positions inside and outside the ordered zone for $K_0 = 10$. For this value, the separatrix between both regimes lies around $Q = 6$. Figure 2 illustrates the crossing of the dashed line in Fig. 1 and the persistence of the negative solution after the disappearance of the other two.

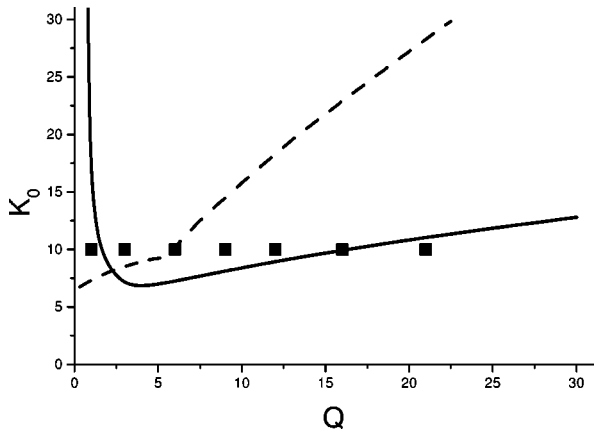

FIG. 1. Phase diagram of the model for $T=2$, $A=0.15$, and $F=0$. The ordered region lies above the full line. Above the dashed line there may exist up to three solutions when $S_m \neq 0$, whereas below it there may exist at most one. The squares represent states at which the shape of $P^{st}(x)$ and the behavior of $\langle \dot{X} \rangle$ as a function of F have been investigated. They correspond to $K_0 = 10$ and $Q = 1$, 3, 6, 9, 12, 16, and 21, respectively.

A. Analysis at constant coupling

Figure 3 shows (for the *true* solution, namely the *stable* $S_m \neq 0$ one) the evolution of $P^{st}(x)$ as a function of Q, for

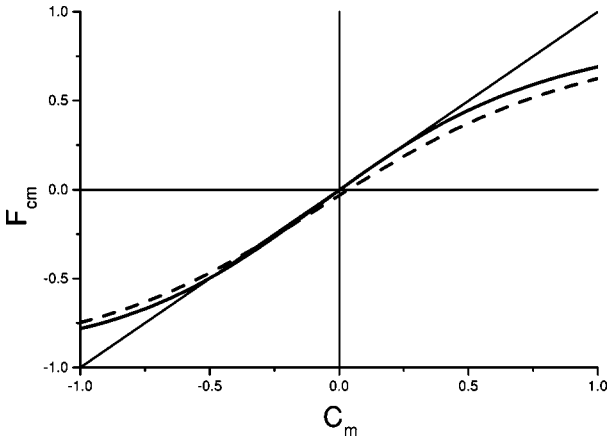

FIG. 2. Illustration of the passage from the IDR to the NDR, as the noise intensity Q increases for $K_0 = 10$ (solid line: $Q = 5.95$; dashed line: $Q = 6.5$). Only the solution with $C_m < 0$ survives after the disappearance of the other two.

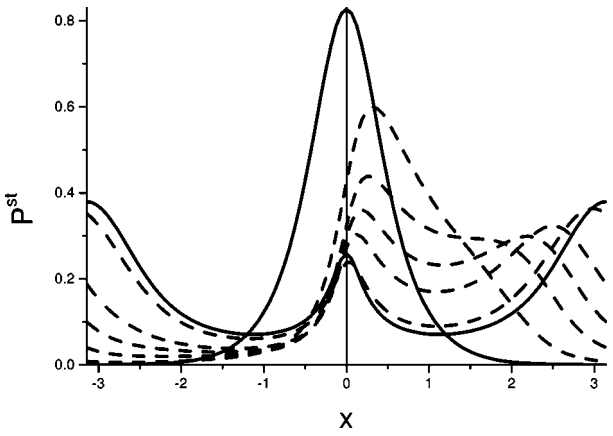

FIG. 3. $P^{st}(x)$ for $K_0=10$ and the values of Q in Fig. 1. For $Q=1$ and $Q=21$ (solid line), it is symmetric, being asymmetric for the remaining values (dashed lines). For Q between 6 and 9, it becomes bimodal and as Q increases, the peak with larger $|x|$ overtakes the other one, although it never reaches beyond 0.5.

$K_0=10$: whereas for $Q=1$ and $Q=21$ it is a *symmetric* function of x, there is a spontaneous breakdown of this symmetry for the remaining values (the system has to choose between two possible *asymmetric* solutions, of which just one is shown). A noticeable feature of $P^{st}(x)$ is that for some $Q>6$ it becomes *bimodal* (in fact, already for $Q=6$ we see an indication that a second peak is developing). According to Fig. 3 and Eq. (17), for $Q<6$ it may be expected that (for the *true* solution) C_m will be positive and even relatively large [however, between $Q=2$ and $Q=6$ other solutions are possible, which lead to other shapes of $P^{st}(x)$ not shown]. As the second peak develops and becomes higher than the original one, C_m shifts toward small negative values (in this region, the one depicted is the only possible solution).

The squares in Fig. 4 plot (always for $K_0=10$) the two possible values of the spontaneous drift velocity $\langle \dot{X} \rangle|_{F=0}$ in the ordered phase as functions of Q. The vertical thick line

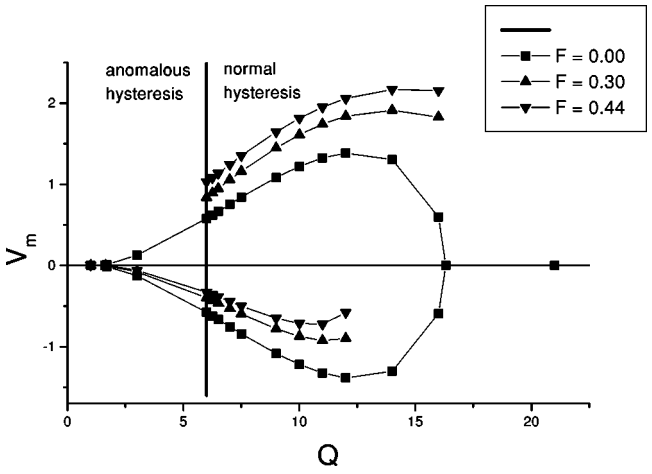

FIG. 4. The order parameter $V_m=\langle \dot{X} \rangle$ (particle current) as a function of Q for $K_0=10$ and $F=0$ (squares), 0.3 (upward triangles), and 0.44 (downward triangles). The vertical thick line signals the transition from anomalous to normal hysteresis.

indicates the value of Q at which the transition from anomalous to normal hysteresis occurs for $K_0=10$. The effect of a moderate positive bias F on $\langle \dot{X} \rangle$ in the normal region (at the right of the thick line) is clearly understandable (the only surprising feature is that on the reentrant branch of the phase boundary, the transition for $F\neq 0$ is so steep that it resembles a first-order one). But the most striking feature is the sudden disappearance of a ''forward'' particle current for the shown values of F as we cross the thick line towards the left (although it may still exist for lower values of F): this is a manifestation of the anomalous hysteresis. As suggested in the first paragraph of this section, this phenomenon is intimately related to the sudden disappearance of some of the multiple solutions when either K_0 or Q are varied in the IDR (see Fig. 2).

Figures 5(a)–5(d) present a sequence of $\langle \dot{X} \rangle$ vs F plots, varying Q across the thick line of Fig. 4. In these, all the solutions to Eqs. (17) and (18) except the one belonging to the branch starting at $C_m\approx 0$ for $S_m=0$ have been included. For $Q=5.97$ [Fig. 5(a)], two (unstable) solutions meet at $\langle \dot{X} \rangle=0$ for $F=0$. The progressive withdrawal of one of them out of the $F\approx 0$ region with increasing Q until its complete disappearance [Figs. 5(b)–5(d)] can be traced back (through their corresponding branches) to the disappearance of solutions for $S_m=0$. Moreover, it is only after this solution has completely disappeared that the stable solution begins to exist for larger values of F and thus normal hysteresis sets in [Fig. 5(d)].

It is also instructive to see how the different branches in Figs. 5(a)–5(c) develop as one enters the ordered region from the left. Figure 6 shows for three points on the $K_0=10$ line the $\langle \dot{X} \rangle$ vs F plots for all the existing solutions (but not the one belonging to the branch starting at $C_m\approx 0$ for $S_m=0$). For $Q=1$, there is a single stable solution displaying negative zero-bias conductance; for $Q=1.7$ (right on the phase boundary) a second (unstable) solution appears and the anomalous hysteretic behavior (clearly seen for $Q=3$) sets in. As suggested by Fig. 4, the situation is different at the reentry: Figure 7 shows that the disappearance of the (normal) hysteretic behavior at the phase boundary in the NDR is in fact abrupt, suggesting a *first-order* phase transition in this regime.

B. Analysis at constant noise intensity

A complementary view of the transition in Figs. 5(a)–5(d) is obtained by varying K_0 at $Q=6.0$ [Figs. 8(a) and 8(b)]: for $K_0=7.25$, a very small normal hysteresis loop can be appreciated, which has grown rather large already for $K_0=8.0$; for $K_0=10.0$, the loop has become anomalous and a third branch has appeared, forming a cusp at the end points of the loop; for a larger K_0 [Fig. 8(b)] the cusp develops into a curl. For larger values of Q (always across the dashed line in Fig. 1), the general pattern is about the same (see Fig. 9 for $Q=9.5$, where the kink of the normal loop at a position rather close to the end point of the anomalous one is suggestive); a similar plot to that in Fig. 2 (but now varying K_0 at $Q=10.0$) is shown in Fig. 10, where the remaining solution displays a

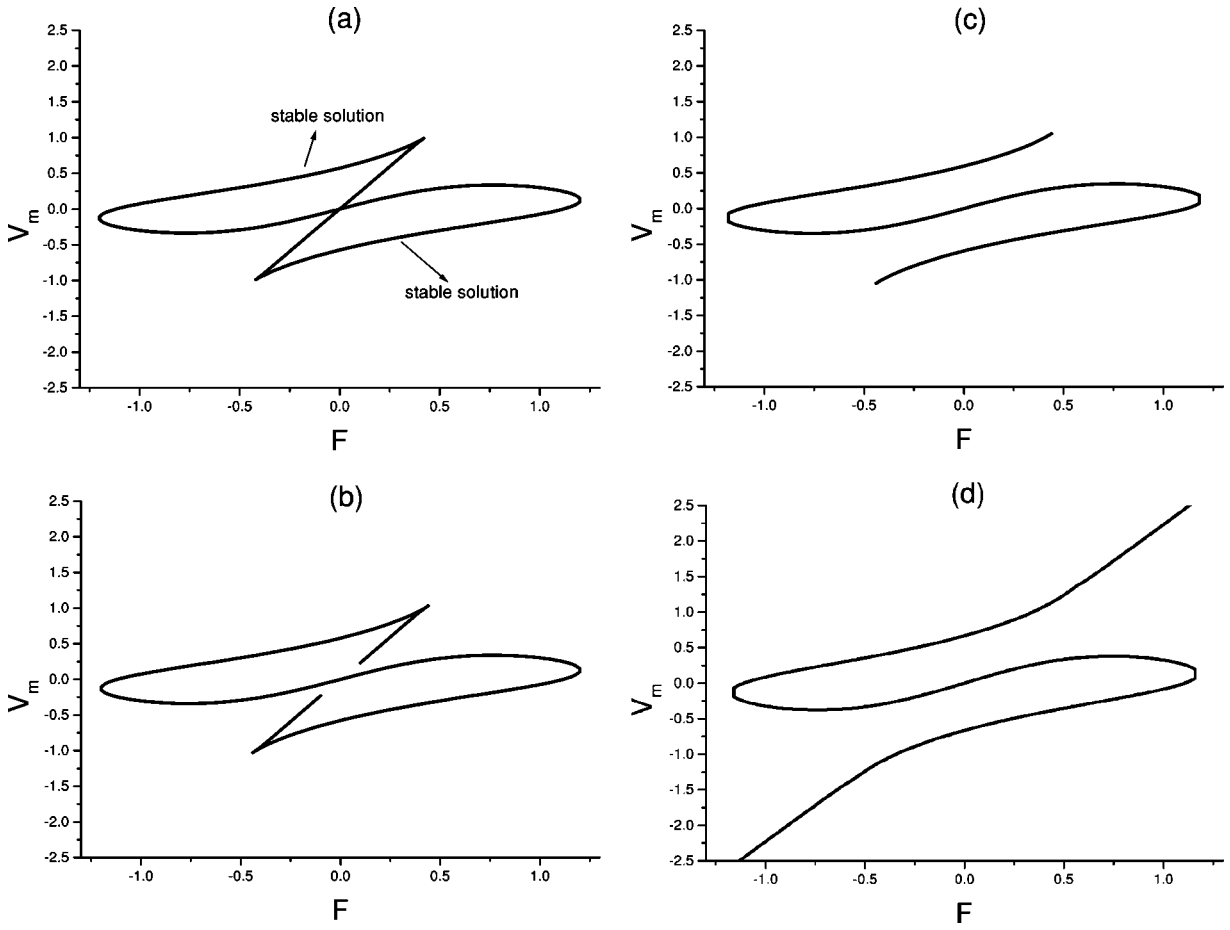

FIG. 5. (a) $V_m=\langle \dot{X} \rangle$ vs F for $K_0=10$ and $Q=5.97$ (just on the left of the dashed line of Fig. 1). The stable solutions are those with larger V_m values; the other two solutions lie on the branches of the $C_m>0$ and $C_m<0$ ones for $S_m=0$ (the solutions with $C_m \approx 0$ are not included). (b) Same as before for $Q=6.0$: one of the unstable solutions has receded from the $F \approx 0$ region (together with the $C_m \approx 0$ one, not shown). (c) Same as before for $Q=6.1$, showing a complete recession from the $F \approx 0$ region. (d) Same as before for $Q=6.5$: not until the dotted line has completely disappeared do solutions in the stable branch appear for $|F|>0.5$ and normal hysteresis sets in.

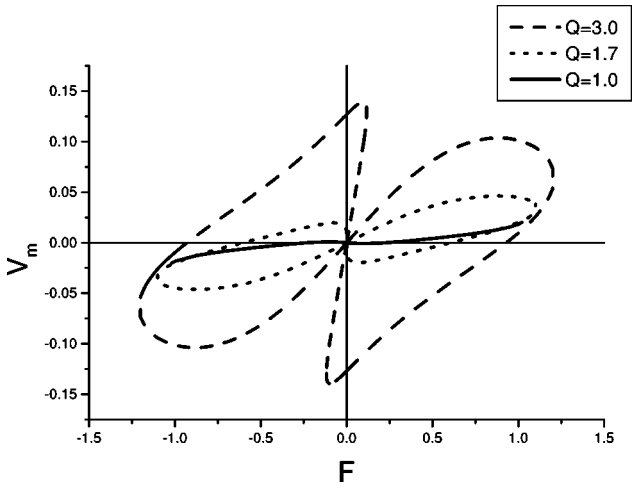

FIG. 6. $V_m=\langle \dot{X} \rangle$ vs F for $K_0=10$ and $Q=1$, 1.7, and 3, illustrating the appearance of multiple solutions and of anomalous hysteresis as the ordered region is reached from the left.

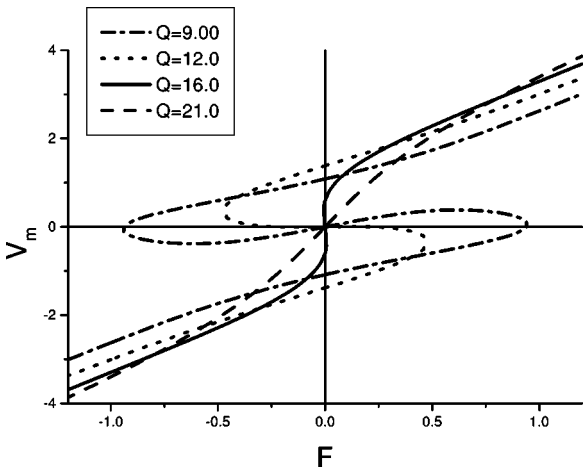

FIG. 7. $V_m=\langle \dot{X} \rangle$ vs F for $K_0=10$ and $Q=9$, 12, 16, and 21, illustrating the disappearance of the normal hysteresis loop at the reentrance (the disordered region is reached from the left).

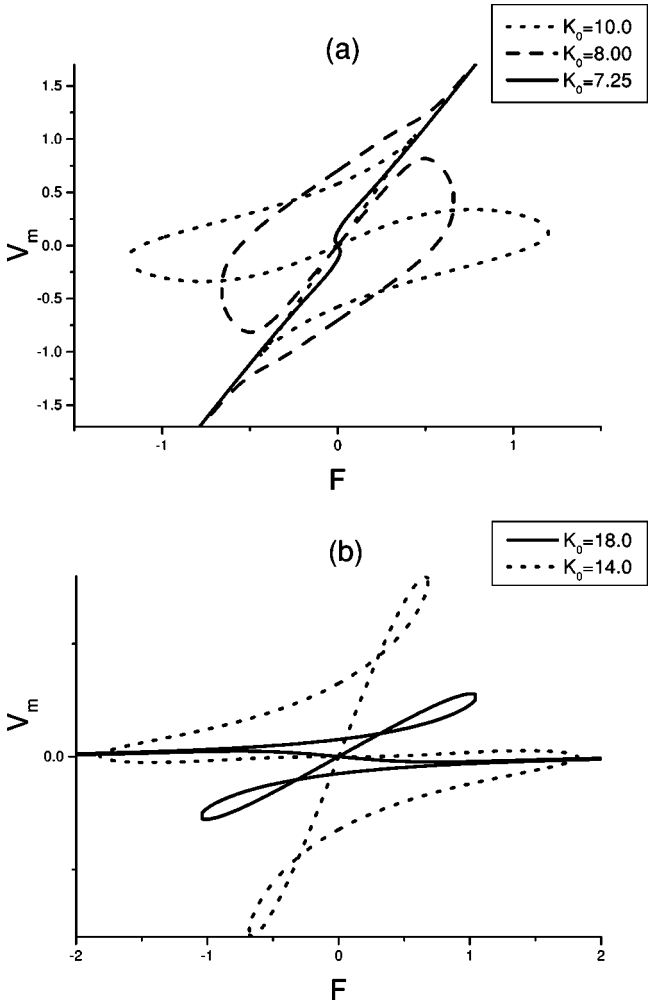

FIG. 8. (a) $V_m=\langle \dot{X} \rangle$ vs F for $Q=6.0$ and $K_0=7.25$, 8.0, and 10.0, illustrating the way the transition from normal to anomalous hysteresis proceeds as K_0 increases at $Q=$const above the dip in Fig. 1. (b) Same as for $K_0=14.0$ and 18.0: the cusp at the end points of the anomalous loop has developed into a curl, thus reducing further its excursion.

larger value of $|C_m|$. Finally, it is interesting to elucidate the nature of the transition *at the left* of the dip in the dashed line in Fig. 1: as Fig. 11 shows, here the loss of two solutions is not accompanied by a change in the character of the hysteresis loop, which remains anomalous.

V. CONCLUSIONS

We have shown the existence of a sharp transition in the behavior of the system inside the ordered phase, from an ''interaction-driven regime'' (IDR) (typically for K_0/Q larger than about three halves) towards a ''noise-driven regime'' (NDR), which differs from the former in several aspects.

(a) Although $\langle \dot{X} \rangle$ shows hysteretic behavior as a function of F everywhere inside the ordered phase, in the IDR its character is *anomalous* (namely clockwise) whereas in the NDR it is *normal* (counterclockwise). Moreover, whereas the height of the anomalous hysteresis loop increases continuously at the phase boundary in the IDR ($\langle \dot{X} \rangle$ acts as an order parameter in a *second*-order phase transition), the disappearance of the normal one proceeds by shrinking its width at a more or less finite height (the transition at the reentry is of *second* order but it is so steep that it resembles a *first*-order one).

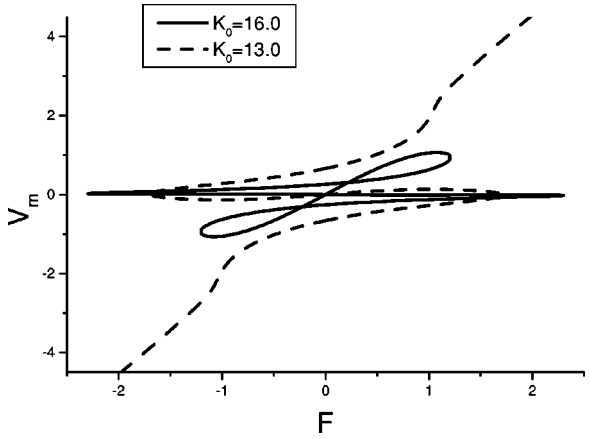

FIG. 9. $V_m=\langle \dot{X} \rangle$ vs F for $Q=9.5$ and $K_0=16.0$ (IDR) and 13.0 (NDR). For $K_0=13.0$, there is still a remnant of the curl existing in the anomalous zone.

(b) The shape of the stationary probability distribution function (PDF) changes *qualitatively* in going from the IDR to the NDR (it becomes *bimodal* and remains so as the disordered region is reentered and the PDF becomes symmetric again, the peak at π then being higher than the one at 0).

(c) Whereas in the IDR there are *several* solutions with $S_m=0$ to the mean-field equations [Eqs. (17) and (18)], in the NDR there is a *unique* solution with $S_m=0$. Solutions of this kind are relevant as a safe starting guess for the Newton-Raphson solution of Eqs. (17) and (18) in the ordered phase, due to the fact that some solutions may suddenly disappear.

Since the transition from anomalous to normal hysteresis in going from the IDR to the NDR is preceded by the disappearance of a pair of solutions with $S_m=0$, the line in the phase diagram at which these disappear (dashed line in Fig.

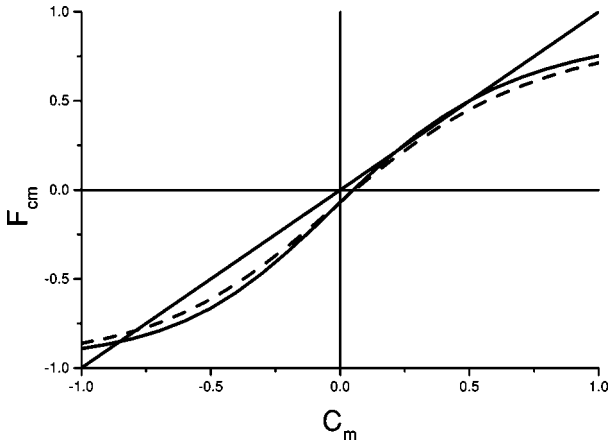

FIG. 10. Illustration of the passage from IDR to NDR, as the coupling K_0 decreases for $Q=10$. As in Fig. 2, only the solution with $C_m<0$ survives after the disappearance of the other two.

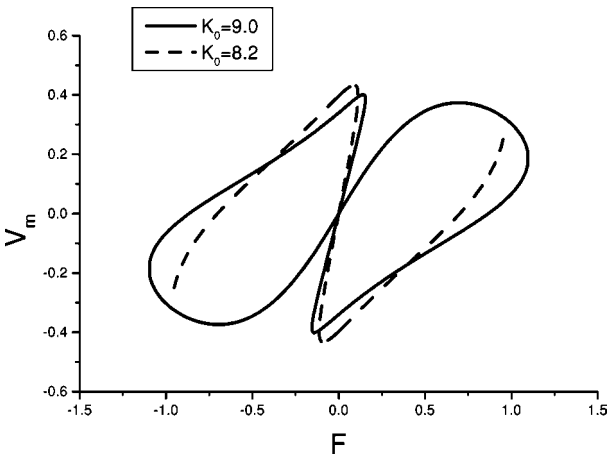

FIG. 11. $V_m=\langle \dot{X} \rangle$ vs F for $Q=4.0$ (at the left of the dip in Fig. 1) and $K_0=9.0$ (IDR) and 8.2 (NDR). One of the branches of unstable solutions has disappeared (together with the $C_m \approx 0$ one, not shown), but the hysteresis loop remains anomalous.

1) *provides an estimation* of the place at which the former transition occurs. Of course, both phenomena are different and so the disappearance of a pair of solutions with $S_m=0$ *does not imply* an anomalous-to-normal transition (recall what happens at the left of the dip in the dashed line of Fig. 1).

Admittedly, all of our results are *mean-field* ones. Although this approximation shows undoubtedly its ability to reveal the richness of the phase diagram of this model, it is reassuring to see that those of our results that are not original do coincide with the numerical simulations for the anomalous hysteresis loop shown in Ref. [5]. Nonetheless, the ultimate verification of these amazing and potentially useful phenomena lies with the experimentalists. We hope to see advances in that direction in the near future.

ACKNOWLEDGMENTS

The authors thank V. Grunfeld for a critical revision of the manuscript. Partial support for this work was provided by the Argentine agencies CONICET (Grant No. PIP 4953/97) and ANPCyT (Grant No. 03-00000-00988).

APPENDIX

1. The stationary probability distribution function

We shall adopt as our standard reference the book by Risken [9], whose equation (3.67) we have written in the form of Eq. (7), with $R(x)$ and $S(x)$ defined in Eqs. (8) and (9). At variance with Risken's choice (and in accord with Ref. [5]) we have adopted $q=1$ in our Eq. (2), equivalent to its Eq. (3.68). Hence Eqs. (3.95) are translated into

$$D^{(1)}(x)=R+\frac{1}{2}SS', \tag{A1}$$

$$D^{(2)}(x)=\frac{1}{2}S^2. \tag{A2}$$

(the prime indicates a derivative with respect to x) whereupon $(D^{(2)})'=SS'$.

The Fokker-Planck equation (4.46) can be written as

$$\partial_t P(x,t)=-\partial_x J(x,t) \tag{A3}$$

with

$$\begin{aligned} J(x,t)&=D^{(1)}(x)P(x,t)-\partial_x[D^{(2)}(x)P(x,t)] \\ &=\left(R+\frac{1}{2}SS'\right)P(x,t)-SS'P(x,t)-\frac{1}{2}S^2\partial_x P(x,t) \\ &=RP(x,t)-\frac{1}{2}S\partial_x[SP(x,t)]. \end{aligned} \tag{A4}$$

On account of Eq. (A4), the stationary case of Eq. (A3) [namely $\partial_t P^{st}(x)=0$] implies $J(x,t)=\text{const}=J$, from which

$$[P^{st}(x)]'=-\frac{2J}{S^2}+\left[\frac{2R}{S^2}-(\ln S)'\right]P^{st}(x). \tag{A5}$$

This equation has the form

$$y'(x)=\alpha(x)+\beta(x)y(x), \tag{A6}$$

and its general solution is

$$\begin{aligned} y(x)=\exp\left[\int_0^x \beta(x')dx'\right]\left\{\int_0^x dx''\alpha(x'')\right. \\ \left.\times\exp\left[-\int_0^{x''}\beta(x')dx'\right]+K\right\}. \end{aligned} \tag{A7}$$

As long as $\alpha(x)\neq 0$, the integration constant K can be chosen so that $y(0)=0$. Otherwise (in our case for $J=0$) the solution is

$$y(x)=K\exp\left[\int_0^x \beta(x')dx'\right]. \tag{A8}$$

If $\alpha(x+L)=\alpha(x)$ and $\beta(x+L)=\beta(x)$, then

$$\int_0^{x+L}\beta(x')dx'=\int_0^L\beta(x')dx'+\int_L^{x+L}\beta(x')dx', \tag{A9}$$

$$\begin{aligned} &\int_0^{x+L}dx''\alpha(x'')\exp\left[-\int_0^{x''}\beta(x')dx'\right] \\ &\quad=\int_0^x dx''\alpha(x'')\exp\left[-\int_0^{x''}\beta(x')dx'\right] \\ &\qquad+\int_x^{x+L}dx''\alpha(x'')\exp\left[-\int_0^{x''}\beta(x')dx'\right]. \end{aligned} \tag{A10}$$

The first term in Eq. (A9) is just a number N and the second equals $\int_0^x \beta(x')dx'$ (as can be seen by writing $x'=x''+L$). Hence

$$y(x+L)=e^N\left\{y(x)+\exp\left[\int_0^x\beta(x')dx'\right]\int_x^{x+L}dx''\alpha(x'')\times\exp\left[-\int_0^{x''}\beta(x')dx'\right]\right\}. \tag{A11}$$

By imposing the boundary condition $y(x+L)=y(x)$,

$$y(x)=\frac{e^N}{1-e^N}\exp\left[\int_0^x\beta(x')dx'\right]\left\{\int_x^{x+L}dx''\alpha(x'')\times\exp\left[-\int_0^{x''}\beta(x')dx'\right]\right\}. \tag{A12}$$

For our case it is $\alpha(x)=-2J/S^2$, $\beta(x)=(2R/S^2)-(\ln S)'$, and $y=P^{st}$, from which by calling

$$\phi(x)=-2\int_0^x\frac{R(x')}{S^2(x')}dx', \tag{A13}$$

$N=-\phi(L)$ holds, and Eq. (A12) reads

$$P^{st}(x)=-\frac{2Je^{-\phi(L)}}{1-e^{-\phi(L)}}\left\{\frac{\exp[-\phi(x)]}{S(x)}\int_x^{x+L}dy\frac{\exp[\phi(y)]}{S(y)}\right\}. \tag{A14}$$

J is fixed by normalization:

$$J=\frac{1-e^{\phi(L)}}{2\int_{-L/2}^{L/2}dx\frac{\exp[-\phi(x)]}{S(x)}\left\{\int_x^{x+L}dy\frac{\exp[\phi(y)]}{S(y)}\right\}}=\frac{1-e^{\phi(L)}}{2\mathcal{N}}. \tag{A15}$$

2. Contribution to $\phi(L)$ of the interparticle interaction

For $0<A<1/4$, $W(x)$ in Eq. (4) has a minimum height $-(1+A)$ at $x=0$ and a maximum height $1-A$ at $x=\pm\pi$. The critical points of its derivative are shifted an amount of order A towards $x=0$ from their $A=0$ position of $x=\pm\pi/2$, and so $S^2(x)$ has its two maxima (of height $1+Q/T$) inside the $\cos x>0$ region. Now $[S(x)]^{-2}$ has two minima of height $(1+Q/T)^{-1}$ in that region, whereas in the $\cos x<0$ one it remains of order 1.

3. Small-x expansion of $\phi(x)$

To first order in y, Eqs. (8) and (10) read $R(y)=-y(1+K_0C_m+4A)+K_0S_m+F$, $S^2(y)=2T[1+(Q/T)(1+4A)^2y^2]$. Hence in this approximation

$$T\phi(x)=\frac{T(1+4A+K_0C_m)}{2Q(1+4A)^2}\ln[1+(Q/T)(1+4A)^2x^2]-\sqrt{T/Q}\,\frac{(K_0S_m+F)}{(1+4A)}\arctan[x\sqrt{Q/T}(1+4A)]\sim(1+4A+K_0C_m)x^2/2-(K_0S_m+F)x. \tag{A16}$$

Assuming $K_0S_m=F=0$, we may approximate

$$P^{st}(x)=\frac{1}{\mathcal{N}}\frac{\exp[-\phi(x)]}{S(x)}\sim\frac{1}{\sqrt{2T\mathcal{N}^2}}\times\exp\left[-\frac{(1+4A+K_0C_m)x^2}{2T}\right]\times\left[1-\frac{Q}{2T}(1+4A)^2x^2\right], \tag{A17}$$

which clearly has a maximum at $x=0$. For small F, the maximum shifts toward $(K_0S_m+F)/(1+4A+K_0C_m)$ and that will in turn produce a small shift in S_m from zero in the direction that the maximum shifts (i.e., that of F), the consequence of which (by the argument in the preceding subsection) is a reversed current.

4. Calculation of the particle current

According to Eq. (3.85) of Ref. [9],

$$D^{(1)}(x,t)=\lim_{\tau\to0}\frac{1}{\tau}\langle X(t+\tau)-X(t)\rangle|_{X(t)=x}=\langle\dot X(t)\rangle|_{X(t)=x} \tag{A18}$$

[in our case, since $D^{(1)}(x)$ does not depend explicitly on time, this is the conditional average over realizations of the noise for any t]. The unrestricted average at time t is then

$$\langle\dot X(t)\rangle=\int_{-L/2}^{L/2}dx\,D^{(1)}(x)P(x,t)=\int_{-L/2}^{L/2}dx\left[R+\frac{1}{2}SS'\right]P(x,t). \tag{A19}$$

From Eq. (A4), it is

$$\langle\dot X(t)\rangle=\int_{-L/2}^{L/2}dx\,J(x,t)+[D^{(2)}(x)P(x,t)]_{-L/2}^{L/2}, \tag{A20}$$

so for *periodic* $P(x,t)$ it is

$$\langle\dot X(t)\rangle=\int_{-L/2}^{L/2}dxJ(x,t) \tag{A21}$$

and in the stationary state, where $J(x,t)=\text{const}=J$,

$$\langle\dot X\rangle=JL. \tag{A22}$$

[1] R. P. Feynman, R. B. Leighton, and M. Sands, *The Feynman Lectures on Physics, Mainly Mechanics, Radiation, and Heat, Volume I* (Addison-Wesley, Reading, MA, 1966), Chap 46.

[2] R. D. Vale and F. Oosawa, Adv. Biophys. **26**, 97 (1990); A. Ajdari and J. Prost, C. R. Acad. Sci., Ser. II: Mec., Phys., Chim., Sci. Terre Univers. **315**, 1635 (1992).

[3] M. O. Magnasco, Phys. Rev. Lett. **71**, 1477 (1993); R. D. Astumian and M. Bier, *ibid.* **72**, 1766 (1994); C. R. Doering, W. Horsthemke, and J. Riordan, *ibid.* **72**, 2984 (1994); R. Bartussek, P. Hänggi, and J. G. Kissner, Europhys. Lett. **28**, 459 (1994).

[4] P. Reimann, Phys. Rep. **290**, 149 (1997).

[5] P. Reimann, R. Kawai, C. Van den Broeck, and P. Hänggi, Europhys. Lett. **45**, 545 (1999).

[6] S. Mangioni, R. Deza, H. S. Wio, and R. Toral, Phys. Rev. Lett. **79**, 2389 (1997); S. Mangioni, R. Deza, R. Toral, and H. S. Wio, Phys. Rev. E **61**, 223 (2000).

[7] C. Van den Broeck, P. Reimann, R. Kawai, and P. Hänggi, in *Statistical Mechanics of Biocomplexity*, edited by D. Reguera, J. M. G. Vilar, and J. M. Rub (Springer-Verlag, Berlin, 1999), pp. 93–111; P. Reimann, C. Van den Broeck, and R. Kawai, Phys. Rev. E **60**, 6402 (1999); J. Buceta, J. M. R. Parrondo, C. Van den Broeck, and J. de la Rubia, *ibid.* **61**, 6287 (2000).

[8] http://www.kawai.phy.uab.edu/research/motor/bm.mov.

[9] H. Risken, *The Fokker-Planck Equation, Methods of Solution and Applications*, 2nd ed. (Springer-Verlag, Berlin, 1989).